

# The power of low-resolution spectroscopy: On the spectral classification of planet candidates in the ground-based CoRoT follow-up

M. Ammler-von Eiff<sup>1,2,\*</sup>, D. Sebastian<sup>1</sup>, E.W. Guenther<sup>1,3</sup>, B. Stecklum<sup>1</sup>, and J. Cabrera<sup>4</sup>

<sup>1</sup> Thüringer Landessternwarte, Sternwarte 5, 07778 Tautenburg, Germany

<sup>2</sup> Max-Planck-Institut für Sonnensystemforschung, Justus-von-Liebig-Weg 3, 37077 Göttingen, Germany

<sup>3</sup> Österreichische Akademie der Wissenschaften, Institut für Weltraumforschung, IWF, Schmiedlstraße 6, 8042 Graz, Austria

<sup>4</sup> Institute of Planetary Research, German Aerospace Center, Rutherfordstrasse 2, D-12489 Berlin, Germany

Received 30 May 2005, accepted 11 Nov 2005

Published online later

**Key words** stars: fundamental parameters — techniques: spectroscopic — Catalogs

Planetary transits detected by the CoRoT mission can be mimicked by a low-mass star in orbit around a giant star. Spectral classification helps to identify the giant stars and also early-type stars which are often excluded from further follow-up. We study the potential and the limitations of low-resolution spectroscopy to improve the photometric spectral types of CoRoT candidates. In particular, we want to study the influence of the signal-to-noise ratio (SNR) of the target spectrum in a quantitative way. We built an own template library and investigate whether a template library from the literature is able to reproduce the classifications. Including previous photometric estimates, we show how the additional spectroscopic information improves the constraints on spectral type. Low-resolution spectroscopy ( $R \approx 1000$ ) of 42 CoRoT targets covering a wide range in SNR (1–437) and of 149 templates was obtained in 2012–2013 with the Nasmyth spectrograph at the Tautenburg 2m telescope. Spectral types have been derived automatically by comparing with the observed template spectra. The classification has been repeated with the external CFLIB library. The spectral class obtained with the external library agrees within a few sub-classes when the target spectrum has a SNR of about 100 at least. While the photometric spectral type can deviate by an entire spectral class, the photometric luminosity classification is as close as a spectroscopic classification with the external library. A low SNR of the target spectrum limits the attainable accuracy of classification more strongly than the use of external templates or photometry. Furthermore we found that low-resolution reconnaissance spectroscopy ensures that good planet candidates are kept that would otherwise be discarded based on photometric spectral type alone.

© 2006 WILEY-VCH Verlag GmbH & Co. KGaA, Weinheim

## 1 Introduction

The CoRoT<sup>1</sup> mission has been the first space mission dedicated to the search for transiting planets (Baglin et al. 2007). Overviews of the mission were given by Baglin et al. (2009), Deleuil et al. (2011), and Moutou et al. (2013). Statistics on candidates and planet detections have been reported for several fields monitored by CoRoT (Cabrera et al. 2009; Carone et al. 2012; Carpano et al. 2009; Cavarroc et al. 2012; Erikson et al. 2012; Moutou et al. 2009).

The goals of ground-based follow-up are manifold (Carone et al. 2012; Carpano et al. 2009), among others the precise derivation of the parameters of a detected planet. While the CoRoT light curve constrains the radius of a planet, ground-based radial-velocity (RV) measurements are needed to derive its mass (Moutou et al. 2009). Only the relative radius and mass of the planet are constrained.

Therefore, the absolute mass and the radius of the host star have to be known very accurately.

False positives play an important role and low-resolution spectroscopy is a step towards their identification. In the case of a false positive, a planetary transit is mimicked by other configurations (Brown 2003). The case of a background eclipsing binary close to the actual target can be resolved by photometry (Almenara et al. 2009; Guenther et al. 2013). The present work aims at another kind of false positive. A planetary transit can be mimicked by a low-mass star orbiting a giant star (see Cavarroc et al. 2012). The identification of giant stars relies on the availability of accurate spectral types.

A first clue about the spectral type of CoRoT targets is given by the CoRoT input catalogue (*ExoDat*<sup>2</sup>; Deleuil et al. 2009) which is based on a massive *UVBr'i'* photometric survey carried out during the mission preparatory phase and has been updated continuously since then. However, in regions of inhomogeneous extinction, it is difficult to obtain spectral class, luminosity class, and extinction simultaneously. Although the photometric classification is

\* Corresponding author: e-mail: ammler@mps.mpg.de

<sup>1</sup> Convection, Rotation & planetary Transits

<sup>2</sup> <http://cesam.oamp.fr/exodat/>

correct on average, it can be deviant for individual stars (Sebastian et al. 2012). Therefore, spectroscopic information is needed to better assess stellar parameters of individual targets (cf. Carone et al. 2012; Gazzano et al. 2010).

Precise information is contained in atmospheric parameters like effective temperature and surface gravity. Those are obtained most accurately from high-resolution spectroscopy (e.g. Gazzano et al. 2013, for CoRoT). As the necessary signal-to-noise ratio (SNR) can be hardly attained at high spectral resolution for faint stars, one needs to resort to low-resolution spectroscopy. Then, a precise measurement of atmospheric parameters is out of reach but spectral classification is still possible.

In practice, spectral classification is done by comparing stellar spectra to template spectra of well-known stars, in particular MK standards. There are different approaches of how to obtain template spectra and to compare them to the target spectra. Computer-based classification has proven efficient. Sebastian et al. (2012) classified more than 10,000 stars in the fields of CoRoT automatically and showed that an accuracy of one to two sub-classes can be achieved. While templates are commonly taken from libraries taken with other instruments (e.g. Gandolfi et al. 2008; Sebastian et al. 2012), the classification is considered most accurate when the templates are taken from an internal library, i.e. have been observed with the same instrument and setup as the target spectra (Gray & Corbally 2009; Wu et al. 2011a). Then, the full spectral range is available for comparison and no convolution is needed to match the spectral resolution.

A low-resolution spectrograph attached to an intermediate-size telescope, like the Nasmyth spectrograph ( $R \approx 1,000$ ) at the Tautenburg 2m telescope, offers a sufficient dynamical range to observe the faint CoRoT targets ( $V < 16$  mag) as well as bright nearby template stars. The Nasmyth spectrograph provides a wide spectral range 360 – 935 nm covering a wealth of stellar features which can be used for classification.

In the present study, we follow the initial work of Guenther et al. (2012) and Sebastian et al. (2012). Based on spectra taken with the Nasmyth spectrograph, we explore the capabilities of low-resolution spectroscopy to derive the spectral types of CoRoT targets. Of course, the accuracy of spectral classification will depend on the signal-to-noise ratio (SNR) of the target spectra. In the course of the follow-up of planet candidates, a large number of stars has to be classified efficiently and to the accuracy required. Since telescope time is limited and the exposure time scales with the square of the SNR, we are interested in a good knowledge of the required SNR.

The CoRoT targets were selected from various internal and public lists, in particular from Deleuil et al. (in preparation)<sup>3</sup>. Most of the CoRoT objects are FGK stars

(Guenther et al. 2012) and these are the most interesting planet host stars. How well does spectral classification distinguish giant stars and dwarf stars, especially at spectral types F, G, and K?

We followed a two-fold approach. Firstly, we followed the canonical approach of spectral classification (Gray & Corbally 2009) and built an internal library of spectral templates with the same spectrograph and setup used to observe the CoRoT targets. Secondly, a classification was done using templates from the Indo-US Coudé-feed library (CFLIB, Valdes et al. 2004), selected for its good coverage of spectral types, luminosity classes, and metallicity. We investigate whether this external library gives similar results. Simultaneously, we analyse the impact of the SNR of the target spectra on the results. In addition, we compare the spectral types obtained to previous photometric classifications given by *ExoDat*. We identify the merits of the inclusion of a spectroscopic classification over a sole photometric classification.

Section 2 explains the selection of stars to build the internal template library. The observation of templates and CoRoT targets is described in Sect. 3. Sect. 4 addresses the data reduction and the coverage of the internal template catalogue is assessed in Sect. 5. We describe the steps of the spectral classification in Sect. 6 and the results in Sect. 7. The results are discussed in Sect. 8 before we conclude in Sect. 9.

## 2 Selecting stars for a new library of template spectra

The template stars need to fulfil a set of requirements. Of course, the spectral types need to be known very well. Having in mind quantitative spectral classification in future work, we adopted as an additional criterion the availability of accurate atmospheric parameters.

Although quantitative classification is beyond of the scope of the present work, we point out here that it has many advantages over the use of spectral types. There is no need to use a conversion scale, e.g. from spectral type to effective temperature which is intrinsically prone to errors. Furthermore, it promises higher precision and flexibility than the classification by spectral type which is limited by the discreteness of the classification scheme. An extension of the traditional grid of spectral types to include metallicity or even abundance patterns would be too demanding. Instead, atmospheric parameters can be used defining a continuous grid which can be sampled by templates according to the requirements of the classification task. For previous work and reviews, see Bailer-Jones (2002); Cayrel et al. (1991); Gray & Johanson (1991); Malyuto et al. (2001); Singh et al. (2002); Stock & Stock (1999).

As another criterion, the template stars should be bright so that spectra can be taken quickly with a high SNR. The

and a discussion of the status of individual candidates is beyond the scope of the present work (but see Deleuil et al.).

<sup>3</sup> The present work includes a statistical study on the type and quality of information available from spectral classification. Therefore, additional follow-up information on particular planet candidates is not included here

templates should cover the range of spectral types of interest. In order to be able to classify most CoRoT targets, we selected templates for early-type and Sun-like stars of different luminosity class from the CFLIB. Wu et al. (2011b) obtained stellar parameters and chemical abundance homogeneously for the CFLIB library.

FGK dwarfs are the best targets to look for planets with CoRoT. To fill the grid with templates, we selected well-studied FGK stars from Fuhrmann (1998-2011). Several of those are MK standards according to Gray & Corbally (2009).

The work of Fuhrmann is restricted to solar-type main-sequence and sub-giant stars. However, in the distant CoRoT fields, the fraction of early-type stars and giants is relatively high. CoRoT covers these luminous stars more completely but there is a lack of cooler main-sequence stars. While early-type stars are covered by the CFLIB, we supplement the set of stellar templates with K giants compiled by Doellinger (2008) who derived the stellar parameters and iron abundance of 62 K giants.

### 3 Observations

All spectra were taken with the low-resolution long-slit spectrograph mounted at the Nasmyth focus of the 2m Alfred Jensch telescope in Tautenburg (Germany). A slit width of 1'' was used to ensure a resolution of  $\approx 1,000$ . The V200 grism was chosen as dispersing element, thus covering the visual wavelength range from 360 to 935 nm. It is a BK7 grism with 300 lines per millimeter and a dispersion of  $225 \text{ \AA mm}^{-1}$ . The detector is a SITE#T4 CCD with  $2048 \times 800$  pixels and a pixel size of  $15 \mu\text{m}$ . We used channel A with a gain of  $1.11 \mu\text{V}$  per electron.

CoRoT monitors several stellar fields consecutively for up to 40 days (short runs) or for up to 150 days (long runs). These fields are selected in two opposite directions in the sky where the galactic plane crosses the equatorial plane. These are the so-called galactic centre and anti-centre-eyes of CoRoT. Seasonal observations of the CoRoT fields are possible in winter (galactic anti-centre) and summer (galactic centre) despite the high latitude of the observing site of  $51^\circ\text{N}$ . The CoRoT fields can be observed at an air mass of approx. 1.5. A total of 42 CoRoT targets covering a brightness range of  $R = 11.0 - 15.5$  was observed in February and July 2012/2013 when the visibility of the CoRoT eyes was best. Table 1 presents the journal of observations.

In addition, we have observed a set of 149 template stars (Table 2). They are bright so that the SNR is high. Exposure times range from a few seconds for the brightest template stars to 30 min for the faintest CoRoT targets. In general, at least two spectra were taken per target in order to remove cosmics. While the usually faint CoRoT targets are observable only under good conditions for a few hours per night, the bright template stars are distributed over the whole sky. They perfectly fill the observing time when CoRoT targets are not visible or when conditions are bad.

**Table 1** Journal of observations sorted by the SNR achieved. The first two columns give the CoRoT and Win identifiers. The Win identifier is composed of the CoRoT run (LR=long run, SR=short run, IR=initial run; a=galactic anti-centre, c=galactic centre; plus a consecutive number), the CCD identifier (E1/E2), and a consecutive number. The run ID identifies the spectroscopic runs carried out in February and July 2012/2013. The  $R$  band magnitude is followed by the number of spectra taken per object. The last column gives the SNR of the co-added spectra.

CoRoT ID	Win ID	run ID	$R$	#	SNR
102634864	LRa01_E1_3221	Feb12	15.2	3	1
102627709	LRa01_E2_1578	Feb12	13.3	1	8
102580137	LRa01_E2_4519	Feb12	15.4	3	16
102698887	LRa01_E1_2240	Feb12	14.2	3	22
616759073	SRa05_E2_3522	Feb12	13.9	3	37
310153107	LRc03_E2_5079	Jul13	14.0	1	40
221699621	SRa02_E1_1011	Feb12	14.0	2	60
310155742	LRc03_E2_5451	Jul13	14.6	3	71
678658629	LRc09_E2_3403	Jul13	14.7	3	71
655228061	LRc09_E2_2479	Jul13	14.5	2	73
631424752	LRc07_E2_2968	Jul13	13.7	2	78
659668516	LRc08_E2_4203	Jul12	14.6	2	80
655049038	LRc09_E2_0892	Jul13	13.9	1	82
659714254	LRc07_E2_4203	Jul13	14.9	3	83
102901032	LRa02_E1_4967	Feb13	15.5	4	89
679896622	LRc09_E2_3338	Jul13	15.2	4	89
632089337	LRc10_E2_3956	Jul13	13.9	2	101
738282899	LRa07_E2_3354	Feb13	15.3	4	103
659676254	LRc08_E2_4520	Jul13	14.6	3	105
102770212	LRa06_E2_5287	Feb13	15.5	4	107
103970832	LRc04_E2_5713	Jul13	15.5	6	109
315219144	SRa03_E2_1073	Feb13	14.5	3	125
104833752	LRc05_E2_3718	Jul12	14.7	5	126
680074530	LRc09_E2_0548	Jul12	13.6	2	126
310170040	LRc03_E2_0935	Jul13	13.8	3	130
633100731	LRc10_E2_5093	Jul13	13.8	4	132
659718186	LRc10_E2_0740	Jul13	13.1	2	134
633496006	LRc10_E2_1984	Jul13	14.5	1	141
659473289	LRc09_E2_0308	Jul12	11.0	1	141
631423929	LRc07_E2_0158	Jul12	12.2	2	179
652180991	LRc08_E2_0275	Jul12	13.3	4	179
21160782	SRc01_E1_0346	Jul13	12.7	1	187
659714295	LRc07_E2_0534	Jul12	12.4	2	196
678656772	LRc09_E2_0131	Jul12	12.3	2	219
652345526	LRc07_E2_0307	Jul12	13.0	4	226
632279463	LRc07_E2_0146	Jul12	12.6	2	240
652312572	LRc07_E2_0182	Jul12	12.0	2	248
105314448	LRc06_E2_0119	Jul12	12.8	4	265
631900113	LRc07_E2_0482	Jul12	12.8	4	277
631423419	LRc07_E2_0187	Jul13	12.3	2	293
104992379	LRc05_E2_0168	Jul12	12.0	2	322
104992379	LRc05_E2_0168	Jul13	12.0	2	437

**Table 2** Stellar templates observed with the Nasmyth spectrograph and their spectral type. The second column gives the run ID which identifies the spectroscopic runs carried out in February and July 2012/2013.

HD number	run ID	spectral type	HD number	run ID	spectral type	HD number	run ID	spectral type
400	Jul12	F8IV	94028	Feb12	F4V	168151	Jul13	F5V
2628	Feb12	A7III	94084	Feb12	K2III	168723	Jul13	K0III-IV
6397	Jul12	F4II-III	95128	Feb12	G1V	170693	Jul13	K1.5III
6920	Jul12	F8V	96064	Feb12	G8V	172340	Jul13	K4III
10362	Feb12	B7II	96833	Jul13	K1III	173667	Feb12	F6V
10476	Jul12	K1V	97989	Feb12	K0III	173936	Feb12	B6V
10697	Jul12	G5IV	98281	Feb12	G8V	175823	Jul13	K5III
12303	Feb12	B8III	99491	Feb12	K0IV	176377	Jul13	G0
12846	Jul12	G2V	100563	Feb12	F5V	176524	Jul13	K0III
12953	Feb12	A1Iae	101501	Feb12	G8V	178187	Feb12	A4III
15318	Feb12	B9III	102328	Feb12	K3III	180554	Feb12	B4IV
30614	Feb12	O9.5Iae	102870	Feb12	F9V	180610	Jul13	K2III
34578	Feb12	A5II	103095	Feb12	G8Vp	182488	Jul13	G8V
35296	Feb12	F8V	104985	Feb12	G9III	182572	Jul13	G8IV
37394	Feb12	K1V	105546	Feb12	G2IIIw	183144	Feb12	B4III
38114	Feb12	G5	105631	Feb12	K0V	184385	Jul13	G8V
39866	Feb12	A2II	110897	Jul12	G0V	184499	Jul12	G0V
41117	Feb12	B2Iaevar	117043	Feb12	G6V	185144	Jul13	G9V
41692	Feb12	B5IV	117176	Feb12	G5V	185269	Jul12	G0IV
43247	Feb12	B9II-III	120136	Jul12	F6IV	186307	Feb12	A6V
43384	Feb12	B3Ib	121560	Feb12	F6V	186408	Jul13	G1.5V
47839	Feb12	O7Ve	122408	Feb12	A3V	186427	Jul13	G3V
47914	Jul13	K5III	127334	Feb12	G5V	186815	Jul13	K2III
48682	Feb12	G0V	128167	Feb12	F2V	187013	Jul12	F7V
50420	Feb12	A9III	130948	Feb12	G1V	187691	Jul13	F8V
51530	Feb12	F7V	132142	Jul12	F7V	187923	Jul13	G0V
52711	Feb12	G4V	132254	Feb12	F7V	187961	Jul12	B7V
55575	Feb12	G0V	136202	Feb12	F8III-IV	188510	Jul12	G5Vw
58855	Feb12	F6V	136729	Feb12	A4V	188512	Jul12	G9.5IV
59747	Feb12	G5V	139323	Feb12	K3V	189944	Feb12	B4V
59881	Feb12	F0III	142373	Jul12	F8Ve	190228	Jul12	G5IV
61295	Feb12	F6II	151862	Feb12	A1V	191243	Feb12	B5Ib
62301	Feb12	F8V	152614	Feb12	B8V	192699	Jul12	G5
63433	Feb12	G5IV	153653	Feb12	A7V	193322	Feb12	O9V
65583	Feb12	G8V	154431	Feb12	A5V	195810	Feb12	B6III
67228	Feb12	G1IV	154445	Feb12	B1V	196504	Feb12	B9V
72946	Feb12	G5V	155514	Feb12	A8V	205139	Feb12	B1II
74280	Feb12	B3V	157214	Jul12	G0V	206827	Jul12	G2V
75732	Feb12	G8V	157681	Jul13	K5III	207970	Jul12	F6IV_Vwvar
76151	Feb12	G3V	158148	Feb12	B5V	208947	Feb12	B2V
82443	Feb12	K0V	158633	Jul12	K0V	210839	Feb12	O6Iab
82621	Feb12	A2V	160290	Jul13	K1III	210855	Jul12	F8V
84737	Feb12	G0.5Va	161797	Jul13	G5IV	212978	Feb12	B2V
85235	Feb12	A3IV	162570	Feb12	A9V	215648	Jul12	F7V
86728	Feb12	G3Va	164136	Feb12	F2II	216385	Jul12	F7IV
88983	Feb12	A8III	164922	Jul12	K0V	218470	Jul12	F5V
89269	Feb12	G5	165401	Jul13	G0V	221830	Jul12	F9V
89744	Feb12	F7V	167042	Jul13	K1III	222794	Jul12	G2V
90277	Feb12	F0V	168009	Jul13	G2V	223385	Feb12	A3Iae
91752	Feb12	F3V	168092	Feb12	F1V			

In order to estimate the bias level and the read-out noise, dark frames were taken with closed shutter and zero exposure time. In order to assess the pixel-to-pixel variation of sensitivity, the wavelength-dependent transmission of the spectrograph, and bad or hot pixels, flat-field frames were taken pointing the telescope to a flat-field screen which is installed in the dome and illuminated by an incandescent lamp.

In principle, the wavelength calibration can be done using sky emission lines in the long-slit spectra. However, the sparseness of sky emission lines in the blue part of the spectra does not permit a precise calibration in this region. It is the blue part of the spectrum which displays a wealth of features and is very valuable for spectral classification. Therefore, spectra of gas discharge lamps (He and Kr) were used for wavelength calibration. At least one set of gas discharge exposures was taken per observing run. A wavelength precision of a few Å is achieved this way and is sufficient for the purpose of spectral classification.

To estimate the signal-to-noise ratio (SNR), we assumed pure photon noise accounting for read-out noise. The total system gain used depends on the amplifier setting chosen. In the present case (setting '20'), we estimated a total system gain of 3.2 electrons per data unit using the full well at the noise roll-over specified by the manufacturer (84,000 electrons)<sup>4</sup>. The readout-noise amounts to 7.8 electrons. This estimate of the SNR is fully sufficient to compare the spectra since all spectra were taken with the same instrument and identical settings. The median is used to distinguish good spectra with high signal and bad spectra with a high noise level.

#### 4 Data reduction

The long-slit spectra have been reduced using the data reduction and analysis system IRAF<sup>5</sup> (Tody 1986, 1993). This procedure comprises bias subtraction, an automatic removal of cosmic rays, and removal of pixel-to-pixel variations by flat-field correction.

All spectra have been wavelength-calibrated using He and Kr spectra. Using IRAF tasks, the wavelengths of prominent lines have been identified and used to derive a wavelength solution which has been applied to all stellar spectra. The spectrograph is mounted at the fork of the telescope so that instrument flexure causes shifts depending on the exact orientation of the telescope. Therefore, sky emission lines have been employed to apply corrections. For each frame with a long exposure time of 20 minutes at least, the sky lines are bright enough to use them as calibration source (Osterbrock et al. 1996). They have been used to derive offsets to correct the wavelength scale. The corrections were small and of the order of the resolution limit.

<sup>4</sup> The full well was scaled to the saturation level obtained at setting '50' and then rescaled to setting '20'.

<sup>5</sup> IRAF is distributed by the National Optical Astronomy Observatories, which are operated by the Association of Universities for Research in Astronomy, Inc., under cooperative agreement with the National Science Foundation.

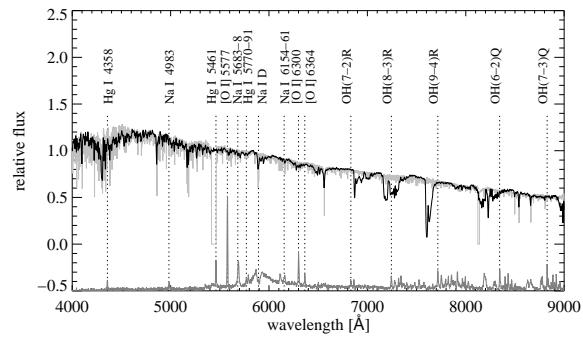


**Fig. 1** The black line shows a Nasmyth spectrum of the G0V star HD 157214. For comparison, a library spectrum with medium resolution (Valdes et al. 2004) is shown (light grey). To match the SED, the template spectrum was used to adjust the flux of the Nasmyth spectrum. Both spectra were normalised to unity at 5550 Å. In addition, the subtracted night sky spectrum of the site is shown (grey) and is offset w.r.t. the stellar spectra for clarity. The most important spectral features are indicated.

The sky background could be subtracted easily from the long-slit spectra. For this purpose, long exposures provide an excellent source to analyse the night-sky emission in Tautenburg. Figure 1 shows the Nasmyth spectrum of a Sun-like star together with the subtracted sky-background.

The most prominent features in the night-sky spectrum are the O I, Hg I, and Na I atomic lines, the broad continuum centred at 5890 Å, and the OH bands in the red part (Osterbrock & Martel 1992; Slanger et al. 2003). These lines originate from the night glow as well as from artificial sources. The broad continuum centered at 5890 Å is characteristic of the presence of artificial light and in this case originates from high-pressure sodium lamps used in the nearby city of Jena, Germany.

The flux calibration of the spectra of CoRoT targets was not possible because of the spectrograph design and the high airmass of CoRoT targets. The orientation of the spectrograph slit cannot be adjusted and the slit-rotation of the spectrograph depends on the hour angle of the object. This leads to a dependency of the detected flux level on atmospheric refraction. In addition, the star is slightly moving on the slit and the exact location on the slit cannot be reproduced. Therefore, the stellar continuum could not be recovered and used for classification. Instead, one has to rely on spectral lines only and the continuum has to be adjusted to match the continuum of the template (Fig. 2). Hence, the comparison is restricted to the strength and the profile of selected absorption lines.

#### 5 The coverage of the new template library

The CFLIB and the new internal template library have many stars in common. 54 CFLIB stars have been included in the

sample chosen from Fuhrmann (1998-2011). The Fuhrmann sample does not cover all spectral types. Therefore, 55 stars have been chosen from the CFLIB catalogue and reobserved for the new library. In total, 109 CFLIB stars have been reobserved.

Within the present work, 149 template spectra of bright stars have been taken. MK spectral types have been adopted from Valdes et al. (2004) when available and from the SIMBAD database otherwise.

Table 3 shows the coverage in spectral type. The catalogue is being filled continuously but a good coverage has already been achieved for dwarf stars. Particularly, FGK dwarfs are densely covered. A finely graduated classification becomes feasible in the FGK regime.

## 6 Computer-based classification

The spectral types of the CoRoT targets have been obtained using a computer-based classification. The software applied (described in Sebastian et al. 2012) compares all target spectra to a library of template spectra. Each target spectrum is matched to template spectra adjusting the radial velocity shift, the level of the continuum, and the slope of the continuum. We selected spectral chunks that contain sensitive lines for spectral classification thus removing parts that are not useful for classification (see Fig. 2). Afterwards the  $\chi^2$  is calculated and compared for each template spectrum. The five best-matching templates are validated by visual inspection. This validation rules out false classifications due to low S/N or stellar activity. The spectral type of the best-matching validated template is adopted for the target spectrum. Guenther et al. (2012) found that the error bar of this classification method depends on the spectral type and the template library used. They analysed the accuracy of the method on a sample of more than 3000 stars and found that the accuracy of this method for low resolution spectra is on average two subclasses. It is slightly better for early-type stars (1.3 subclasses) and less accurate for solar-type stars (2-3 subclasses). The classification is not affected by rotational broadening since the spectral resolution of the Nasmyth spectrograph is too low.

Firstly, we used the internal template library taken with the Nasmyth spectrograph. In the second approach, we used a set of 281 template spectra provided by CFLIB (Valdes et al. 2004)<sup>6</sup>. To compare the CoRoT target spectra directly with the CFLIB templates, we have to ensure that the resolution, the wavelength range, and the continuum flux level are roughly the same. Since the Nasmyth spectra have been taken with a resolution of  $\sim 5 \text{ \AA}$  FWHM (at  $5500 \text{ \AA}$ ), we convolved the CFLIB templates ( $\sim 1 \text{ \AA}$  FWHM) with a Gaussian kernel.

For the comparison with internal templates, the full wavelength range from  $3600$  to  $9350 \text{ \AA}$  can be used in

**Table 3** The coverage of the new template library in spectral type. At each spectral type, the number of templates is given.

spectral class	luminosity class						
	I	II	II-III	III	III-IV	IV	V
O6	1						
O7							1
O9							1
O9.5	1						
B1		1					1
B2	1						2
B3	1						1
B4				1		1	1
B5	1					1	1
B6				1			1
B7		1					1
B8				1			1
B9			1	1			1
A1	1						1
A2		1					1
A3	1					1	1
A4				1			1
A5		1					1
A6							1
A7				1			1
A8				1			1
A9				1			1
F0				1			1
F1							1
F2		1					1
F3							1
F4			1				1
F5							3
F6		1				2	3
F7						1	6
F8					1	1	6
F9							2
G0						1	8
G0.5							1
G1						1	2
G1.5							1
G2				1			4
G3							3
G4							1
G5						4	8
G6							1
G8						1	8
G9				1			1
G9.5						1	
K0				2	1	1	4
K1				3			2
K1.5				1			
K2				3			
K3				1			1
K4				1			
K5				3			

<sup>6</sup> These CFLIB templates have a high SNR of 100 at least and cover almost the full range of spectral types.

principle since the target spectra have been obtained with the same spectrograph. However, especially the red part of the covered wavelength region contains telluric bands. The strength of these bands is variable. Although a correction of telluric bands is possible in principle, the scarcity of useful features does not justify this effort. The strongest telluric oxygen bands appear at 6884 Å (Catanzaro 1997). Therefore, the wavelength region applied here starts in the blue at 3950 Å where we get sufficient signal and ends at 6800 Å at the blue edge of the oxygen bands. In the extreme red, there is a very short range of  $\approx 400$  Å not strongly affected by telluric absorption. This region contains three prominent CaII lines (8498, 8542, and 8662 Å) at almost all spectral types which can be used for spectral classification (Gray & Corbally 2009). For early-type stars, some H I lines of the Paschen series were included in addition. In spite of some night-sky emission lines that could affect the spectra (see Fig. 1), we chose the region from 8400 to 8880 Å in addition to the blue part (4200 – 6800 Å) for comparison (Fig. 2). For spectra with low SNR, we had to set the blue edge to 4800 Å to skip the blue part with very low signal.

When using the external CFLIB templates, the wavelength range is limited to the overlapping region of the CoRoT target spectra and the CFLIB templates. In particular, the very red part with the Ca II triplet and the Paschen series cannot be used. Moreover, parts with strong telluric absorption had to be excluded again and once more, the wavelength range had to be reduced to 4800 – 6850 Å in the case of noisy spectra.

The design of the spectrograph does not allow one to reproduce the continuum flux (Sect. 4) so that the continuum flux could not be used for classification. Therefore, the CoRoT spectra and the Nasmyth templates were normalised and seven chunks (five in the case of low SNR, resp.) were compared separately (Fig. 2). This way, the influence of the unknown absolute flux level and the extinction was optimally removed. This method ensures that the spurious continuum flux levels of both spectra do not distort the results of the classification.

The CFLIB templates are not flux-calibrated either but Valdes et al. (2004) recovered the SED of the CFLIB spectra from spectrophotometric templates. In order to compare the Nasmyth spectra and the CFLIB templates, they were normalised again in an appropriate way and compared in different chunks.

Figure 2 shows the comparison of a CoRoT target to its best-matching Nasmyth template. In this case, the target spectrum matches the spectrum of HD 121560 perfectly (spectral type F6V).

## 7 Results

The results of the classification are listed in Table 4. First of all, there are some interesting qualitative findings. In neither case, the best-matching external template originates from the same star as the best-matching internal template, in spite

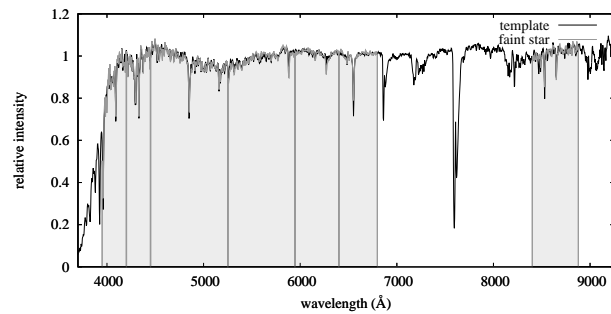


**Fig. 2** Comparison of a target spectrum (grey line) with the best-matching template (black line). The vertical lines mark the borders of chunks which are compared separately and used to adjust the continuum level of the spectra.

of a high number of stars common to both libraries. Also it occurs that an external template spectrum matches another CoRoT object. The CFLIB spectrum of HD 120136 matches LRC05\_E2\_3718 while the Nasmyth spectrum of HD 120136 matches the spectrum of LRC07\_E2\_0182. Apparently, the CFLIB spectrum of HD 120136 is as different from the Nasmyth spectrum as is the difference between the spectra of LRC07\_E2\_0182 and LRC05\_E2\_3718. Although both stars are late-F or early-G type stars, we note, that the SNR of the spectrum of LRC05\_E2\_3718 is only half of that of LRC07\_E2\_0182. Interestingly, the Nasmyth spectrum of HD 84737 matched Nasmyth spectra of as many as five CoRoT objects. Again, the SNR is obviously important since all the five target spectra suffer from low signal!

The qualitative discussion above shows that the SNR plays a role. A more quantitative presentation of the data confirms that the agreement depends on the noise level of the CoRoT target spectra (Fig. 3(a)). Fig. 4 presents another view on the data by projecting along the noise axis and showing the distribution of the residuals separately for the good and bad spectra. The spread tends to increase with decreasing signal, i.e. the strongest discrepancies are usually encountered for spectra of least quality. At highest signal, the discrepancies tend to vanish.

The mean difference in spectral type is as low as 2 subclasses when considering the good spectra only. Remarkably, hardly any systematic offsets or trends are seen in our sample.

The distribution of residuals appears far from normal in the case of the bad spectra. In the case of the good spectra, however, an identification of outliers seems possible. There are two outliers in spectral type, LRC09\_E2\_0308 and LRC05\_E2\_3718. The deviation cannot be readily explained since the SNR is reasonably good.

The spectroscopic classifications were compared with photometric classifications taken from the online version of *ExoDat* as of May 16<sup>th</sup>, 2014. We note that the scatter is increased for bad spectra (Figs. 3(b), 3(c)). But even for good spectra, the scatter is dramatically larger and we note that photometry tends to assign earlier spectral types. The level

**Table 4** Results of spectral classification (sorted by SNR). The table contrasts the classification obtained via two different sets of templates – the internal library obtained by us with the Nasmyth spectrograph and the template library of Valdes et al. (2004) (CFLIB). LRC10\_E2\_1984 is an M star for which no template was taken with the Nasmyth spectrograph.

Win ID	SNR	spec. type (Exodat)	templates taken with the Nasmyth spectrograph		templates taken from Valdes et al. (2004)	
			templ.	spec. type	templ.	spec. type
LRa01_E1_3221	1	A5V	HD139323	K3V	HD190390	F1III
LRa01_E2_1578	8	A5V	HD210855	F8V	HD158352	A8V
LRa01_E2_4519	16	A5IV	HD136729	A4V	HD173495	A1V+
LRa01_E1_2240	22	A5V	HD61295	F6II	HD150453	F3V
SRa05_E2_3522	37	O5V	HD136729	A4V	HD177724	A0Vn
LRc03_E2_5079	40	G5II	HD47914	K5 III	HD232078	K3IIp
SRa02_E1_1011	60	F8IV	HD102870	F9V	HD16673	F6V
LRc03_E2_5451	71	K3I	HD99491	K0IV	HD34255	K4lab:
LRc09_E2_3403	71	G8V	HD84737	G0.5Va	HD177249	G5.5IIb
LRc09_E2_2479	73	K0III	HD47914	K5 III	HD178717	K3.5III:
LRc07_E2_2968	78	G5III	HD184385	G8V	HD5286	K1 IV
LRc08_E2_4203	80	A0V	HD2628	A7III	HD186377	A5III
LRc09_E2_0892	82	K5III	HD160290	K1III	HD175306	G9 IIIb
LRc07_E2_4203	83	G0IV	HD84737	G0.5Va	HD39833	G0 III
LRa02_E1_4967	89	A5IV	HD128167	F2V	HD204363	F7V
LRc09_E2_3338	89	A0V	HD136729	A4V	HD177724	A0 Vn
LRc10_E2_3956	101	K2III	HD84737	G0.5Va	HD191615	G8 IV
LRa07_E2_3354	103	A2V	HD39866	A2II	HD168270	B9V
LRc08_E2_4520	105	A5IV	HD84737	G0.5Va	HD128987	G6V
LRa06_E2_5287	107	G0IV	HD168151	F5V	HD150453	F3V
LRc04_E2_5713	109	A5IV	HD165401	G0V	HD130948	G1 V
SRa03_E2_1073	125	F8V	HD91752	F3V	HD56986	F0IV
LRc05_E2_3718	126	F8IV	HD84737	G0.5Va	HD120136	F6IV
LRc09_E2_0548	126	F8IV	HD10697	G5IV	HD128987	G6V
LRc03_E2_0935	130	G0V	HD215648	F7V	HD204363	F7 V
LRc10_E2_5093	132	K0III	HD170693	K1.5III	HD5286	K1 IV
LRc10_E2_0740	134	K3III	HD157681	K5III	HD34255	K4lab:
LRc10_E2_1984	141	—	—	—	HD126327	M7.5 III
LRc09_E2_0308	141	B1V	HD157214	G0V	HD115617	G5V
LRc07_E2_0158	179	F8IV	HD216385	F7IV	HD136064	F9IV
LRc08_E2_0275	179	G8V	HD192699	G5	HD76813	G9III
SRc01_E1_0346	187	A0V	HD41692	B5IV	HD168199	B5 V
LRc07_E2_0534	196	G5III	HD180610	K2III	HD112127	K2.5III
LRc09_E2_0131	219	G0V	HD168723	K0III-IV	HD149661	K2V
LRc07_E2_0307	226	F5IV	HD173667	F6V	HD150012	F5IV
LRc07_E2_0146	240	F0V	HD210855	F8V	HD136064	F9IV
LRc07_E2_0182	248	A5V	HD120136	F6IV	HD61064	F6III
LRc06_E2_0119	265	F8IV	HD187013	F7V	HD59380	F8V
LRc07_E2_0482	277	A5IV	HD215648	F7V	HD62301	F8V
LRc07_E2_0187	293	F8IV	HD215648	F7V	HD59380	F8 V
LRc05_E2_0168	322	F8IV	HD176377	G0	HD39587	G0V
LRc05_E2_0168	437	F8IV	HD176377	G0	HD39587	G0V

of agreement is the same whatever the choice of the template library - internal or external.

Sebastian et al. (2012) showed that for solar-type stars the computer-based spectral classification cannot distinguish between main-sequence stars and sub-giants but between main-sequence stars and giants or super-giants. Therefore, we distinguish giant-like (I, II, III, III-IV) and dwarf-like luminosity classes (IV, V); also because of the low numbers in the present work. The luminosity classification based on the two different sets of templates is compared in a statistical sense (Table 5). Each field contains the number of CoRoT targets with corresponding classifications. Again, good and bad spectra are distinguished. The total number of good(bad) spectra is 21(20). 15(10) stars

are dwarf-like according to either set of templates while there is agreement on a giant-like luminosity class for 2(4) stars. Still, there is substantial disagreement for 4(6) stars. Two(four) dwarf-like stars are given giant-like classifications when using the CFLIB templates and 2(2) giant-like stars are assigned dwarf-like classifications. In summary, only 19% of the classifications of good spectra are not reproduced by the external library compared to 30% of the classifications of the bad spectra.

The contingency tables are reproduced for the comparisons with the photometric classification from *ExoDat* (Tables 6, 7). When comparing the internal library with *ExoDat*, there are 1(6) off-diagonal elements. Comparing the CFLIB to *ExoDat*, there are 3(6) off-diagonal elements.



**Table 5** Contingency table showing the agreement of luminosity classifications obtained with the external CFLIB template library and the internal Nasmyth library. The number of classifications based on good spectra is shown and succeeded in brackets by the number of classifications based on bad spectra. Good and bad spectra are distinguished using the median of the SNR (cf. Fig. 3). The solid lines in the table divide giant-like classes and dwarf-like classes.

CFLIB templates	Nasmyth templates					
	I	II	III	III-IV	IV	V
I			1		(1)	
II			(1)			(1)
III			1(3)		1	1(2)
III-IV						
IV			1		1	4(2)
V		(2)		1	2	8(8)

**Table 6** Contingency table showing the agreement of spectroscopic and photometric luminosity classifications: internal Nasmyth catalogue vs. photometric Exodat classification. The layout follows Table 5.

Exodat	Nasmyth templates					
	I	II	III	III-IV	IV	V
I					(1)	
II			(1)			
III			3(2)			(2)
III-IV						
IV					2	8(6)
V		(2)	(1)	1	2	5(5)

**Table 7** Contingency table showing the agreement of spectroscopic and photometric luminosity classifications: CFLIB catalogue vs. photometric Exodat classification. The layout follows Table 5.

Exodat	CFLIB templates					
	I	II	III	III-IV	IV	V
I	(1)					
II		(1)				
III	1		1(2)		1(2)	
III-IV						
IV			(1)		3	7(5)
V		(1)	2(2)		2	4(5)

For an update of the status of CoRoT candidates with a spectroscopic classification, we recommend a rather conservative approach in order to not discard planet candidates prematurely. For the present sample and for the discussion below, we adopt a giant-like luminosity class only in the case that both template libraries yield a giant-like classification. Five out of these 6 stars were classified giants by photometry, too. Furthermore, we identified seven early-type stars (F3 or earlier), six out of these also early-type according to *ExoDat*.

However, there is disagreement in several cases. Intriguingly, seven stars are early-type according to photometry but late-type according to spectroscopy, affecting almost half of

the photometric early-type targets. Furthermore, 2 out of 9 giants are actually dwarf stars. There is no single late-type star which turned out early-type. Only one early-type dwarf turned out a giant.

## 8 Discussion

We obtained target and template spectra with the same instrument in order to avoid any systematic effects which might be introduced by the use of another instrument. This involves a major effort since a large number of spectral types has to be covered. As many as 149 template stars have been observed to cover different luminosity classes and chemical abundance patterns. Although the coverage is not yet complete, it is very dense.

One of the main goals was to find out whether an external template catalogue, here the CFLIB, can be used to reproduce the results of a classification with an internal library. The best-matching template stars found in the present work show that the outcome mainly depends on the SNR of the target spectra. At sufficiently high SNR ( $\geq 100$ ), the mean difference in spectral type is still within the internal uncertainties of the method of a few sub-classes (Guenther et al. 2012; Sebastian et al. 2012). Also a discrepancy of the luminosity classification occurred more often in the case of bad target spectra. Although this assessment is based on small numbers, too, it ascribes at least part of the discrepancy to noise.

The agreement in spectral class for good target spectra gives high confidence in the use of external templates. In contrast, the photometric classification deviates by up to an entire spectral class. Nevertheless, as the scatter w.r.t. photometry increases for spectra with bad SNR, we conclude - as is expected - that the spectral classification is not able to provide accurate spectral types if the signal is too low. The photometric *ExoDat* classification of luminosity performs as well as a spectral classification employing the external library. In this respect, the present work extends the work of Sebastian et al. (2012) who derived spectral types from AAO spectra using templates from CFLIB and who compared the results to *ExoDat* classifications.

The comparison of the spectroscopic and photometric classifications shows that photometry favours early-type classifications (cf. Fig. 3). Half of them turned out late-type stars which is roughly in line with the findings of Sebastian et al. (2012) who showed that 30% of the photometric A and B stars are actually late-type stars. Planet search campaigns often remove early-type targets from the list of candidates since the radial velocity follow-up of such objects can be challenging. Moreover, the low-resolution spectroscopy was able to identify 2 dwarf stars among 9 photometric giants. Giant stars are excluded from follow-up since the transit signature would be due to a low-mass star rather than a planet. This way, low-resolution spectroscopy can recover good candidates among early-type targets (50%) and giant stars (25%) discarded otherwise. For

the present work, we studied 17 late-type dwarf stars which are particularly interesting for follow-up. None of these turned out a giant so that photometry performs much better in this case.

## 9 Summary and Conclusions

Within the ground-based follow-up of CoRoT targets we took low-resolution spectra of 42 objects with the low-resolution Nasmyth spectrograph in Tautenburg.

The spectra of the CoRoT targets were classified using two different sets of templates, an internal template library taken with the same instrument as the target spectra and the external CFLIB library. Although the internal library comprises spectra of 149 stars, the coverage is not fully complete and will be complemented in upcoming observing runs. The use of the new set of templates to refine preliminary classifications is intriguing. The new template grid is densest in the regime of F and G dwarfs which is most promising for planet detections with CoRoT.

We found that the use of external library spectra yields similar results when the signal-to-noise ratio of the target spectrum is sufficiently high ( $\geq 100$ ). However, the luminosity classification with an external library does not perform better than a photometric classification. Therefore, it seems feasible to resort to a less costly photometric luminosity classification when an internal template library is not available.

As an aside, we know the atmospheric parameters of the matching templates. Therefore, a quantitative classification by atmospheric parameters becomes feasible, including effective temperature and surface gravity along with chemical abundances. This might disentangle the well-known degeneracy in spectral classification due to unknown metallicity that may certainly affect the present work. Also, the follow-up of transit-planet candidates would benefit a lot from quantitative classification. However, there are major uncertainties. At first, systematic tests will be needed to assess the accuracy of the quantitative spectral classification, e.g. by reproducing the atmospheric parameters of stars selected from the template library.

The present work highlights the importance of spectroscopic follow-up of CoRoT candidates when only a photometric classification has been available before. With modern multi-object spectrographs at hand (e.g. AAO, LAMOST), low-resolution spectroscopic characterisation should become an indispensable part of any effort to follow-up on planet candidates identified in wide-field surveys.

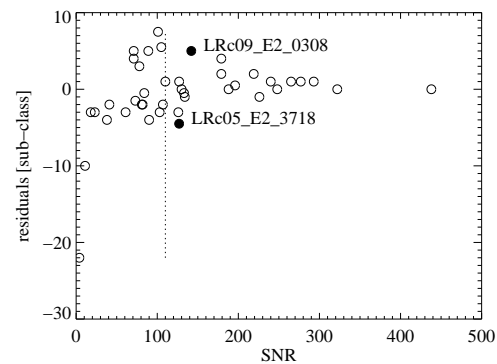
**Acknowledgements.** The selection of CoRoT targets is based on contributions by P. Bordé, F. Bouchy, R. Diaz, S. Grziwa, G. Montagnier, and B. Samuel within the detection and ground-based follow-up of CoRoT candidates. M.A. was supported by DLR (Deutsches Zentrum für Luft-und Raumfahrt) under the project 50 OW 0204. We would like to thank the workshops and the night assistants at the observatory in Tautenburg, Germany. This research has made use of the ExoDat Database, operated at LAM-OAMP,

Marseille, France, on behalf of the CoRoT/Exoplanet program. This research has made use of the SIMBAD database, operated at the CDS, Strasbourg, France, and NASAs Astrophysics Data System Bibliographic Services.

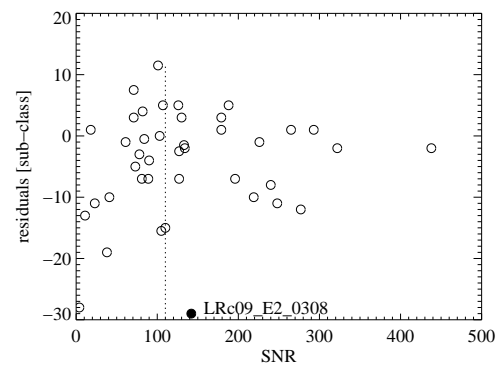
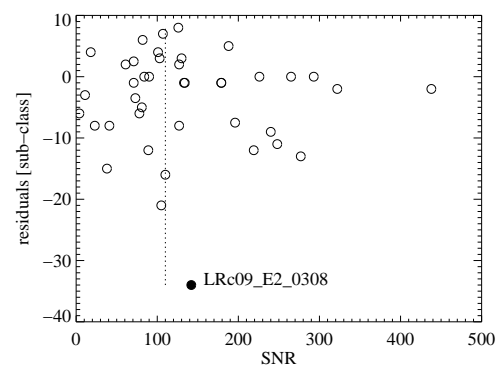
## References

- Almenara, J. M., Deeg, H. J., Aigrain, S., et al.: 2009, *A&A* 506, 337
- Baglin, A., Auvergne, M., Barge, P., et al.: 2009, in *IAU Symposium*, Vol. 253, IAU Symposium, ed. F. Pont, D. Sasselov, & M. J. Holman, 71–81
- Baglin, A., Auvergne, M., Barge, P., et al.: 2007, in *American Institute of Physics Conference Series*, Vol. 895, Fifty Years of Romanian Astrophysics, ed. C. Dumitrache, N. A. Popescu, M. D. Suran, & V. Mioc, 201–209
- Bailer-Jones, C. A. L.: 2002, in *Automated Data Analysis in Astronomy*, ed. R. Gupta, H. P. Singh, & C. A. L. Bailer-Jones, 83
- Brown, T. M.: 2003, *ApJ* 593, L125
- Cabrera, J., Fridlund, M., Ollivier, M., et al.: 2009, *A&A* 506, 501
- Carone, L., Gandolfi, D., Cabrera, J., et al.: 2012, *A&A* 538, A112
- Carpano, S., Cabrera, J., Alonso, R., et al.: 2009, *A&A* 506, 491
- Catanzaro, G.: 1997, *Ap&SS* 257, 161
- Cavarrac, C., Moutou, C., Gandolfi, D., et al.: 2012, *Ap&SS* 337, 511
- Cayrel, R., Perrin, M.-N., Barbuy, B., & Buser, R.: 1991, *A&A* 247, 108
- Deleuil, M., Meunier, J. C., Moutou, C., et al.: 2009, *AJ* 138, 649
- Deleuil, M., Moutou, C., & Bordé, P.: 2011, *Detection and Dynamics of Transiting Exoplanets*, St. Michel l'Observatoire, France, Edited by F. Bouchy; R. Díaz; C. Moutou; EPJ Web of Conferences, Volume 11, id.01001, 11, 1001
- Doellinger, M.: 2008, PhD thesis, LMU München: Fakultät für Physik
- Erikson, A., Santerne, A., Renner, S., et al.: 2012, *A&A* 539, A14
- Fuhrmann, K.: 1998, *A&A* 338, 161
- Fuhrmann, K.: 2000, [http://www.usm.uni-muenchen.de/people/gehren/topics/pap\\_100.pdf](http://www.usm.uni-muenchen.de/people/gehren/topics/pap_100.pdf)  
[www.ing.iac.es/klaus/pap\\_100.ps](http://www.ing.iac.es/klaus/pap_100.ps)
- Fuhrmann, K.: 2004, *AN* 325, 3
- Fuhrmann, K.: 2008, *MNRAS* 384, 173
- Fuhrmann, K.: 2011, *MNRAS* 414, 2893
- Gandolfi, D., Alcalá, J. M., Leccia, S., et al.: 2008, *ApJ* 687, 1303
- Gazzano, J.-C., de Laverny, P., Deleuil, M., et al.: 2010, *A&A* 523, A91
- Gazzano, J.-C., Kordopatis, G., Deleuil, M., et al.: 2013, *A&A* 550, A125
- Gray, D. F. & Johanson, H. L.: 1991, *PASP* 103, 439
- Gray, R. O. & Corbally, J., C.: 2009, *Stellar Spectral Classification* (Princeton University Press)
- Guenther, E. W., Fridlund, M., Alonso, R., et al.: 2013, *A&A* 556, A75
- Guenther, E. W., Gandolfi, D., Sebastian, D., et al.: 2012, *A&A* 543, A125
- Malyuto, V., Lazauskaite, R., & Shvelidze, T.: 2001, *NewA* 6, 381
- Moutou, C., Deleuil, M., Guillot, T., et al.: 2013, *Icarus* 226, 1625
- Moutou, C., Pont, F., Bouchy, F., et al.: 2009, *A&A* 506, 321
- Osterbrock, D. E., Fulbright, J. P., Martel, A. R., et al.: 1996, *PASP* 108, 277
- Osterbrock, D. E. & Martel, A.: 1992, *PASP* 104, 76

- Sebastian, D., Guenther, E. W., Schaffenroth, V., et al.: 2012, A&A 541, A34
- Sheen, Y.-K. & Byun, Y.-I.: 2004, JKAS 37, 87
- Singh, H. P., Bailer-Jones, C. A. L., & Gupta, R.: 2002, in Automated Data Analysis in Astronomy, ed. R. Gupta, H. P. Singh, & C. A. L. Bailer-Jones, 69
- Slanger, T. G., Cosby, P. C., Osterbrock, D. E., Stone, R. P. S., & Misch, A. A.: 2003, PASP 115, 869
- Stock, J. & Stock, J. M.: 1999, RMxAA 35, 143
- Tody, D.: 1986, in Society of Photo-Optical Instrumentation Engineers (SPIE) Conference Series, Vol. 627, Society of Photo-Optical Instrumentation Engineers (SPIE) Conference Series, ed. D. L. Crawford, 733–+
- Tody, D.: 1993, in Astronomical Society of the Pacific Conference Series, Vol. 52, Astronomical Data Analysis Software and Systems II, ed. R. J. Hanisch, R. J. V. Brissenden, & J. Barnes, 173
- Valdes, F., Gupta, R., Rose, J. A., Singh, H. P., & Bell, D. J.: 2004, ApJS 152, 251
- Wu, Y., Luo, A.-L., Li, H.-N., et al.: 2011a, RAA 11, 924
- Wu, Y., Singh, H. P., Prugniel, P., Gupta, R., & Koleva, M.: 2011b, A&A 525, A71+



(a) external templates (CFLIB) - internal templates

(b) photometric classification (*ExoDat*) - internal templates(c) photometric classification (*ExoDat*) - external templates (CFLIB)

**Fig. 3** Residuals of classifications when using external templates and photometric classifications. The difference of spectral types (in sub-classes) is displayed vs. the SNR. The vertical line shows the median SNR found in Sect. 3, and is used to distinguish good and bad spectra. The  $2\sigma$  outliers among the good spectra are highlighted by filled circles and discussed in the text.

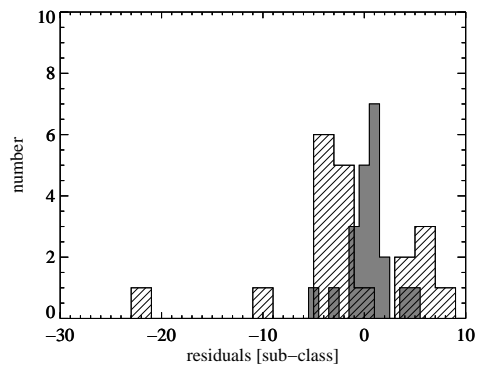


**Fig. 4** Histogram of residuals of classifications when using the CFLIB library (corresponding to Fig. 3(a)). The difference of spectral types is shown in units of sub-class. The filled style distinguishes spectra with good (grey) and bad signal (hatched) according to the division line shown in Fig. 3.